

# State of the art in electromagnetic modeling for the Compact Linear Collider

Arno Candel<sup>1</sup>, Andreas Kabel, Lie-Quan Lee, Zenghai Li, Cho Ng,  
Greg Schussman and Kwok Ko

SLAC National Accelerator Laboratory, Menlo Park, CA 94025, USA

E-mail: <sup>1</sup> [candel@slac.stanford.edu](mailto:candel@slac.stanford.edu)

**Abstract.** SLAC's Advanced Computations Department (ACD) has developed the parallel 3D electromagnetic time-domain code T3P for simulations of wakefields and transients in complex accelerator structures. T3P is based on state-of-the-art Finite Element methods on unstructured grids and features unconditional stability, quadratic surface approximation and up to 6<sup>th</sup>-order vector basis functions for unprecedented simulation accuracy. Optimized for large-scale parallel processing on leadership supercomputing facilities, T3P allows simulations of realistic 3D structures with fast turn-around times, aiding the design of the next generation of accelerator facilities. Applications include simulations of the proposed two-beam accelerator structures for the Compact Linear Collider (CLIC) – wakefield damping in the Power Extraction and Transfer Structure (PETS) and power transfer to the main beam accelerating structures are investigated.

## 1. Introduction

Particle accelerators have been essential tools of scientific discovery for decades. Future linear e+e- colliders operating at the next energy frontier above 1 TeV are expected to complement the Large Hadron Collider (LHC) and lead to further insights which reach far beyond the Standard Model in particle physics. Such accelerators are among the world's largest, most complex facilities and their system requirements continually push the envelope of accelerator science and technology.

The construction and operation costs of next-generation linear colliders have become almost prohibitive, and simple scaling of previous accelerator designs to larger energies might not be optimal. Innovative designs can significantly improve the price/performance ratio. For example, the Compact Linear Collider (CLIC) design improves the power transfer efficiency of accelerating energy to the particle beam.

The CLIC is a design study for a future e+e- collider based on normal-conducting X-band (12 GHz) technology. The current CLIC design consists of two accelerators, one providing the other with RF power. A low energy, high-current drive beam passes through the passive Power Extraction and Transfer Structures (PETS) and supplies intense electromagnetic fields to the accelerating structures for the main beam. The conventional technology, based on klystrons, is only used to power the drive beam. Figure 1 shows the layout of one basic unit of the two-beam accelerator which is replicated many thousand times for each of the two 21 kilometer-long CLIC linacs. For this novel two-beam accelerator scheme to work, numerous technical problems must first be resolved (e.g., RF breakdown and dark current issues at high power and high

*Submitted to the Journal of Physics: Conference Series*

*Invited talk presented at SciDAC 2009, 06/14/2009 -- 06/18/2009, San Diego, CA*

*Work supported in part by US Department of Energy contract DE-AC02-76SF00515*

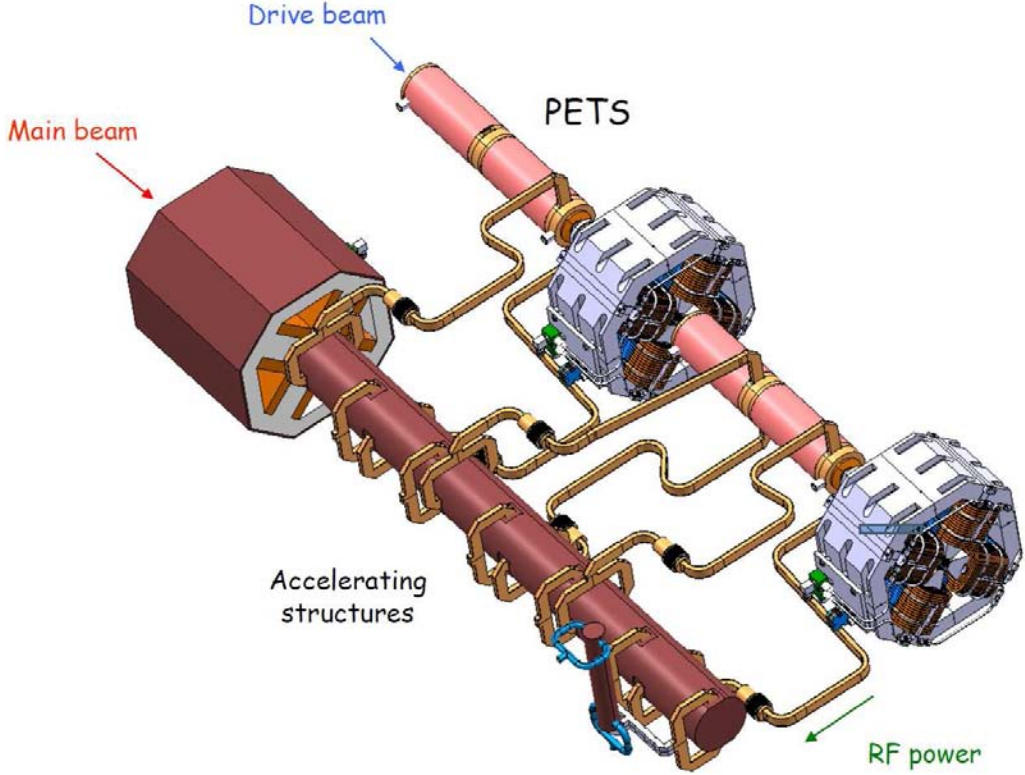


**Figure 1.** Compact Linear Collider two-beam accelerator: RF power to accelerate the main beam in the accelerating structures is provided by a high current drive beam passing through the power extraction and transfer structures (PETS). Each PETS is connected to two accelerating structures through waveguides. Schematic courtesy of CERN.

gradients, wakefield damping and coupling between the PETS and the accelerator structures, etc.). Thorough understanding of these challenges is essential for the accelerator R&D to develop a more cost-effective and reliable design. A strong collaborative effort between multiple research labs has been put forward to address these issues through numerical and experimental means.

This paper presents our contribution as part of the CLIC R&D effort. We have devoted our focus to the analysis of wakefield effects in the PETS and accelerator structures through advanced computing. In the PETS structure, high drive beam current requirements can lead to strong wakefields. If these wakefields are not dissipated, they can cause drive beam instabilities. Further, parasitic fields propagating between the PETS and accelerator structures may cause harmful effects to the main colliding beams and need to be mitigated in the design. We use the time-domain code T3P from the parallel Finite Element code suite ACE3P to study these transient effects.

Section 2 outlines the numerical methods used in T3P, and sections 3 and 4 present numerical validation results of wakefield damping and power transfer in the CLIC two-beam accelerator structures.

## 2. Parallel electromagnetic time-domain code T3P

The simulation code T3P solves the full set of Maxwell's equations in the time domain and includes retardation and boundary effects from first principles. T3P uses unstructured meshes of curved (second-order) tetrahedral elements for modeling of small geometric features and

scattering effects with high accuracy. In combination with higher-order field representation (up to 6<sup>th</sup> order), unprecedented simulation accuracy is obtained through efficient use of computational resources.

In our approach, Ampère's and Faraday's laws are combined and integrated over time to yield the inhomogeneous vector wave equation for the time integral of the electric field  $\mathbf{E}$ :

$$\left( \varepsilon \frac{\partial^2}{\partial t^2} + \sigma_{\text{eff}} \frac{\partial}{\partial t} + \nabla \times \mu^{-1} \nabla \times \right) \int^t \mathbf{E} \, d\tau = -\mathbf{J}, \quad (1)$$

with permittivity  $\varepsilon = \varepsilon_0 \varepsilon_r$  and permeability  $\mu = \mu_0 \mu_r$ . In the current implementation, a constant value of the effective conductivity  $\sigma_{\text{eff}} = \tan\delta \cdot 2\pi f \cdot \varepsilon$  is assumed by fixing a frequency  $f$ , and the losses are specified by the loss tangent  $\tan\delta$ . As is common for wakefield computations of rigid beams, the electric current source density  $\mathbf{J}$  is given by a one-dimensional Gaussian particle distribution, moving at the speed of light along the beam line.

The computational domain is discretized into curved tetrahedral elements and  $\int^t \mathbf{E} \, d\tau$  in Eq. (1) is represented as an expansion in hierarchical Whitney vector basis functions  $\mathbf{N}_i(\mathbf{x})$

$$\int^t \mathbf{E}(\mathbf{x}, \tau) \, d\tau = \sum_{i=1}^{N_p} e_i(t) \cdot \mathbf{N}_i(\mathbf{x}), \quad (2)$$

up to order  $p$  within each element. For illustration, the numbers of basis functions for first, second and sixth order are  $N_1 = 6$ ,  $N_2 = 20$  and  $N_6 = 216$ , respectively. Higher-order elements (both curved and with higher-order basis functions) not only significantly improve field accuracy and dispersive properties [1], but also generally lead to higher-order accurate particle-field coupling equivalent to, but much less laborious than, complicated higher-order interpolation schemes commonly found in finite-difference methods.

The Galerkin method is used for spatial discretization. The resulting set of global expansion coefficients  $e_i$  represents the field degrees of freedom (DOFs) of the system. The Newmark-Beta scheme is employed for temporal discretization, where  $t = n \cdot \Delta t$ :

$$\begin{aligned} \left( \mathbf{M} + \frac{\Delta t}{2} (\mathbf{R} + \mathbf{Q}) + \beta (\Delta t)^2 \mathbf{K} \right) \mathbf{e}^{n+1} &= (\Delta t)^2 (\beta \mathbf{f}^{n+1} + (1 - 2\beta) \mathbf{f}^n + \beta \mathbf{f}^{n-1}) \\ &+ \left( 2\mathbf{M} - (1 - 2\beta) (\Delta t)^2 \mathbf{K} \right) \mathbf{e}^n - \left( \mathbf{M} - \frac{\Delta t}{2} (\mathbf{R} + \mathbf{Q}) + \beta (\Delta t)^2 \mathbf{K} \right) \mathbf{e}^{n-1} \end{aligned} \quad (3)$$

with matrices

$$\begin{aligned} M_{i,j} &= \int \varepsilon \mathbf{N}_i \cdot \mathbf{N}_j \, d\Omega, & Q_{i,j} &= \int \frac{1}{c\mu} (\mathbf{n} \times \mathbf{N}_i) \cdot (\mathbf{n} \times \mathbf{N}_j) \, dS, \\ R_{i,j} &= \int \sigma_{\text{eff}} \mathbf{N}_i \cdot \mathbf{N}_j \, d\Omega, & K_{i,j} &= \int \frac{1}{\mu} (\nabla \times \mathbf{N}_i) \cdot (\nabla \times \mathbf{N}_j) \, d\Omega, \\ \text{and rhs vector} & \quad f_i = \int \mathbf{N}_i \cdot \mathbf{J} \, d\Omega. \end{aligned}$$

Solution of the implicit system (3) with a linear solver leads to an unconditionally stable scheme for  $\beta \geq 0.25$  [2], where the largest allowable time step does not depend on the smallest mesh size in the overall computational domain. However, it is reasonable to use corresponding scales for the discretization of time and space. The simulation time step  $\Delta t$  determines the temporal field resolution, and both the local mesh size  $h$  and the local order of the basis functions  $p$  determine the spatial resolution of the fields. Depending on the local speed of light and the resulting wave numbers for the frequency range of interest, static or adaptive  $hp$ -refinement of both the mesh size and the basis order can significantly improve the modeling accuracy.

The electric field  $\mathbf{E}$  and the magnetic flux density  $\mathbf{B}$  are easily obtained from the solution vector  $\mathbf{e}(t)$  at a given (discrete) time  $t$ :

$$\mathbf{E}(\mathbf{x}, t) = \sum_i \partial_t e_i(t) \cdot \mathbf{N}_i(\mathbf{x}) \quad \text{and} \quad \mathbf{B}(\mathbf{x}, t) = - \sum_i e_i(t) \cdot (\nabla \times \mathbf{N}_i)(\mathbf{x}). \quad (4)$$

T3P is optimized for large-scale parallel operation on leadership supercomputing facilities, and the performance is mostly dominated by the scalability of the linear solver used for the field updates. Due to the large memory requirements of direct solvers, large-scale problems are typically solved with iterative methods (e.g., the conjugate gradient (CG) algorithm in combination with suitable preconditioners). Figure 2 shows the strong scalability of T3P on a Cray XT4 system.

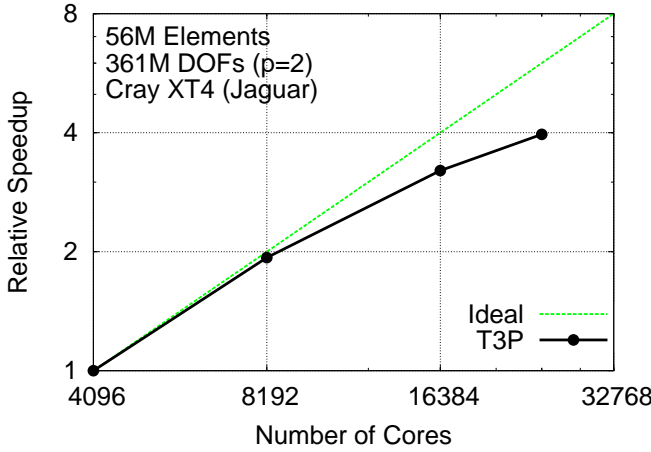


**Figure 2.** Strong scalability of T3P on the Jaguar Cray XT4 system for a problem with 360M DOFs, normalized to a reference run on 4096 cores with about 18 seconds of walltime per time step. The scalability is dominated by the linear solver for the field updates (here: CG with incomplete Cholesky preconditioner).

More detailed information about the employed methods, validation, and applications of T3P have been published earlier [3, 4, 5, 6].

### 3. PETSc wakefield damping calculations

The PETSc is a periodically loaded traveling wave structure with an active length of 21.3 cm, a period of 6.253 mm and an aperture of 23 mm. It is assembled from 8 identical sectors separated by radial slots with embedded lossy dielectric loads to dampen the transverse wakefields.

Figure 3 shows a detailed view of a high-quality mesh model of the PETSc with 34 regular cells, 2 matching cells, an outer tank and the output coupler. A model of one symmetric quadrant of the PETSc requires roughly 9 million tetrahedral elements, with an average mesh resolution of below 1 mm in the vacuum region and 0.3 mm for the dielectric loads ( $\epsilon_r=24$ ,  $\mu_r=1$ ) which require a locally refined mesh for proper resolution of the smaller resulting wavelengths. Using this PETSc mesh model, wakefield calculations have been performed with T3P. It is sufficient for purposes of this study to only model one symmetric quarter of the structure. To excite transverse dipole wakefields, a rigid Gaussian beam is driven along the  $z$ -direction with an  $x$ -offset of 2.5 mm, in combination with electric boundary conditions on the  $yz$ -symmetry plane, and magnetic (symmetric) boundary conditions on the  $xz$ -symmetry plane. The beam profile has a length of  $\sigma_z=2$  mm and is truncated at  $\pm 5\sigma_z$ . For simplicity, the same basis order  $p$  is used for all mesh elements and the effective conductivity is calculated with  $f=12$  GHz, see Eq. (1).

Figure 4 shows one half of the structure with a snapshot of the dipole wakefields excited by the transit of the beam. The wake potential is a measure of how much a trailing particle is deflected by the wakefields caused by a leading bunch when passing through the structure. It is

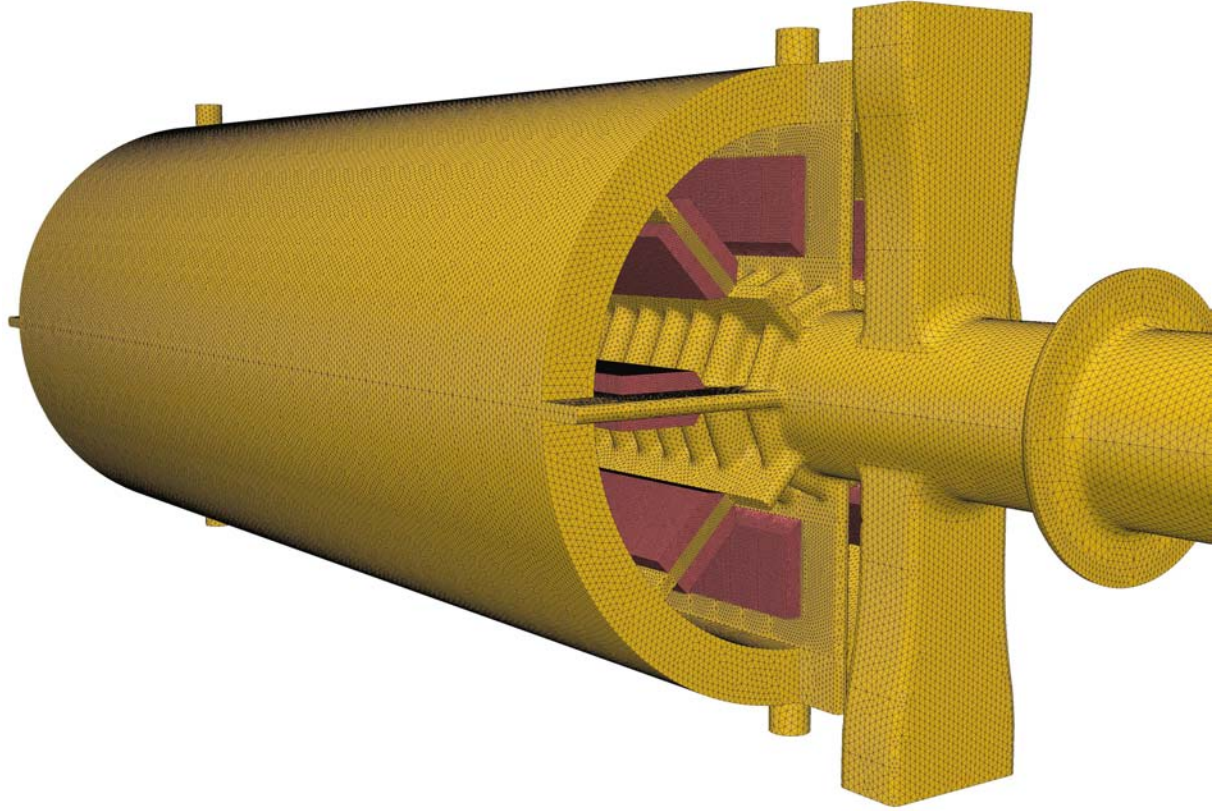


**Figure 3.** External view of the unstructured conformal tetrahedral mesh model of the PETs. For T3P calculations, only one symmetric quadrant consisting of approx. 9 million tetrahedral quadratic elements is used. The drive beam travels from left to right. The dielectric loads are highlighted in red and the corresponding mesh region is locally refined for improved resolution of the smaller resulting wavelengths.

defined as the work performed by the wakefields on the trailing particle of unit charge during transit through the structure:  $w = \int_{-\infty}^{\infty} (\mathbf{E} + \mathbf{v} \times \mathbf{B}) dz$ . It depends on the cavity geometry, the distance from the leading bunch, and the charge and offset of the leading bunch. The transverse wake potential is typically normalized by the leading bunch charge and offset.

Figure 5 shows the convergence of the transverse wake potential as a function of the order  $p$  of the Finite Element basis functions used in T3P calculations, and fast convergence is observed. Figure 6 shows the convergence behavior of the transverse impedance, the Fourier transform of the wake potential of a point charge. Figure 7 shows the effect of the lossy dielectric loads by comparing the transverse wake potential with and without losses ( $\tan\delta=0.32$  vs.  $\tan\delta=0$ , c.f. Eq. (1)). The dielectric properties and permeability of the absorber material are kept constant (i.e.,  $\epsilon_r=24$ ,  $\mu_r=1$ ). A drop of about one order of magnitude in the wakefield amplitudes is observed after about one active length if dissipation losses are included in the simulation.

For both the wake potential and the impedance, results from  $p=1$  calculations are the least accurate and show differences to calculations with  $p=2$  and  $p=3$ , which are almost identical. In a previous study [6] with a slightly simplified geometry, T3P results were compared to results obtained with the commercial parallel finite-difference code GdfidL, and good general agreement between the codes was found. As expected for a conventional finite-difference code, based on a structured mesh and cut-cell boundary approximation, GdfidL results show similar deviations to the converged results as the T3P results obtained with  $p=1$ .

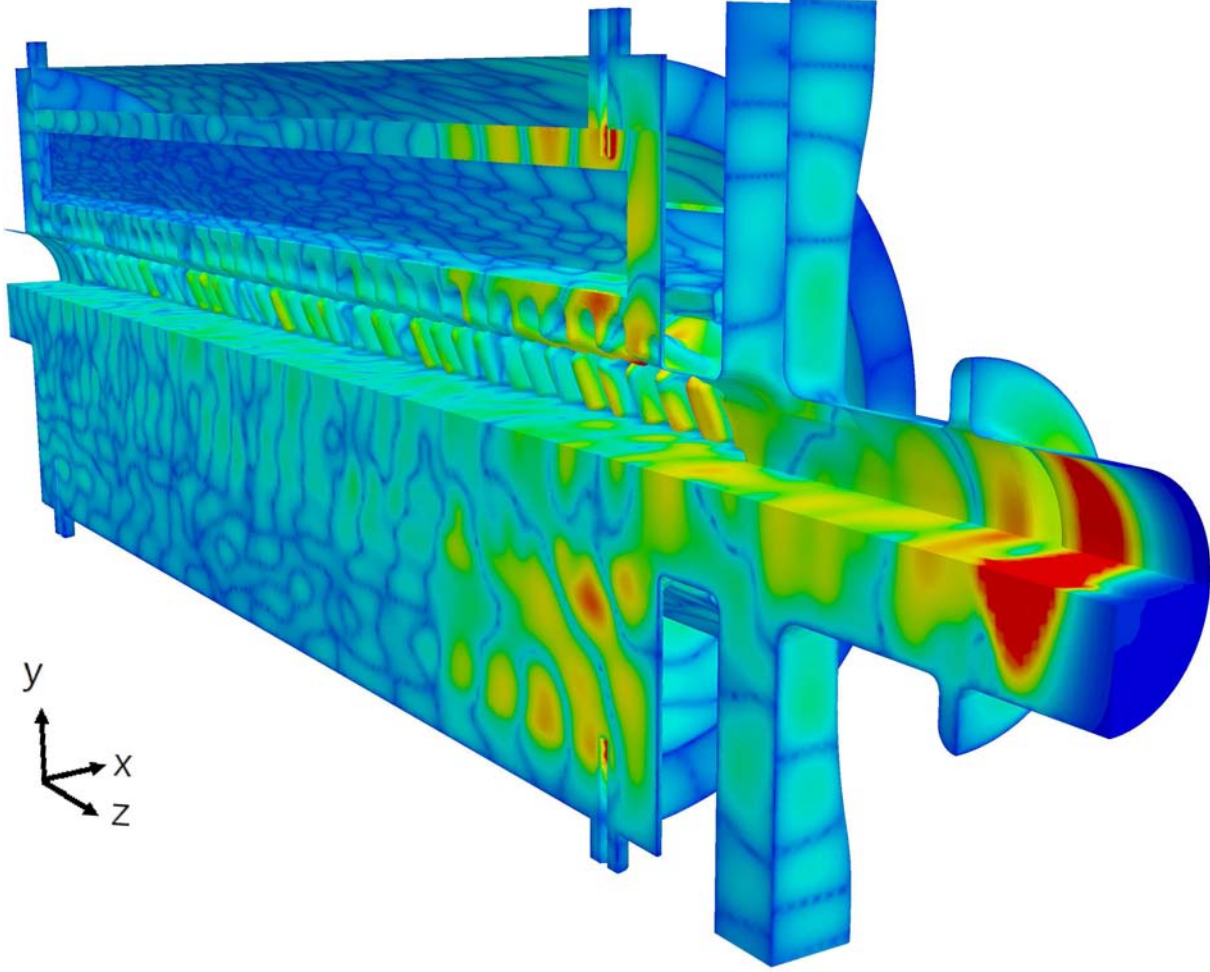


**Figure 4.** Snapshot of excited dipole wakefields in the PETS, as calculated with T3P. The electric field magnitude is shown in a cut view. On the bottom half, the fields on the symmetry planes are shown as well, and the beam with an offset of  $x=2.5$  mm is visible near the end of the PETS. Strong damping in the lossy dielectric loads ( $\epsilon_r=24$ ,  $\tan\delta=0.32$ ) is directly observed, as well as some fields in the output coupler and choke.

Table 1 shows the runtime parameters for the PETS wakefield damping simulations with T3P for  $p=1\dots 3$ , performed on the Jaguar Cray XT4 machine at NCCS. The time scale for wakefield

**Table 1.** Runtime parameters for the PETS wakefield damping studies with T3P.

Basis Order	Degrees of Freedom	CPUs	Walltime/step
p=1	10M	1152	0.30 secs
p=2	54M	1152	1.63 secs
p=3	159M	4096	10.6 secs

damping in the PETS is on the order of several nanoseconds. Consequently, meaningful results for  $p=1$  can be obtained within a few hundred CPU hours, while  $p=3$  requires in the order of a

## PETS Wake Potential, Loads: $\varepsilon_r=24$ , $\tan\delta=0.32$

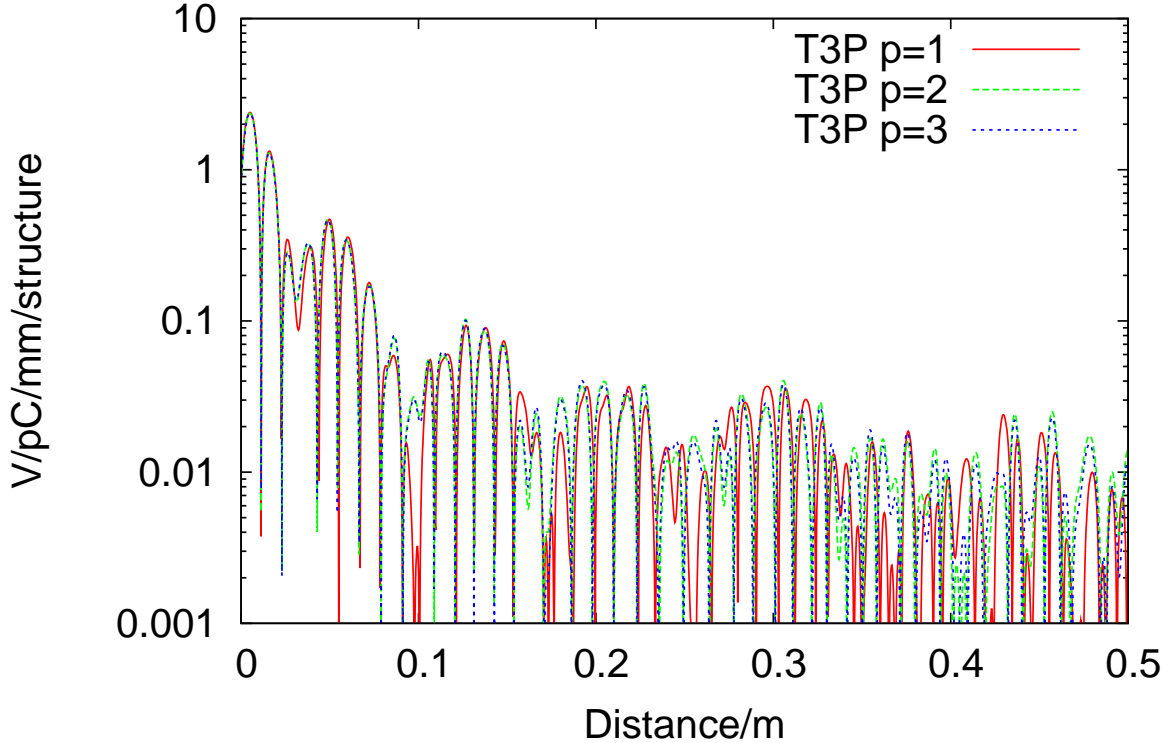


**Figure 5.** Convergence of transverse wake potential in the PETS as a function of the order  $p$  of the Finite Element basis functions used in T3P calculations. A Gaussian dipole current of  $\sigma_z=2$  mm is used to excite the wakefields.

hundred thousand CPU hours. Results with  $p=2$  require on the order of ten thousand CPU hours and represent a reasonable compromise in terms of accuracy vs. computational requirements.

For wakefield damping calculations with  $p=2$ , a simulation time step of 0.5 picoseconds is sufficient to reach convergence in the results. This time step corresponds to a wavelength of 150 microns and frequencies in the terahertz range. It is small enough to model both the frequency content of the beam ( $\sigma_z=2$  mm), and the smallest features in the geometry with high accuracy.

#### 4. Power transfer from PETS to the accelerating structures

The previous section has shown that T3P is able to reach numerical convergence in the wakefield damping results for the PETS. It is now conceivable for the first time to perform numerical simulations of a coupled structure of both the PETS and the accelerating structure in great detail.

In recent years evidence has been found that the maximum sustainable gradient in an accelerating structure depends on the RF power flow through the structure. The high-gradient CLIC accelerating structures are consequently designed to have a very low group velocity, in the order of only 2% of the speed of light, which results in long filling times. To obtain useful simulation results, control of numerical dispersion errors and long-term stability are essential.

Figure 8 shows the simulation model used for T3P calculations of the power transfer from the PETS to the accelerating structure. A total of 18M tetrahedral elements are used to discretize the coupled structures. In the present study, fundamental mode power transfer from the PETS

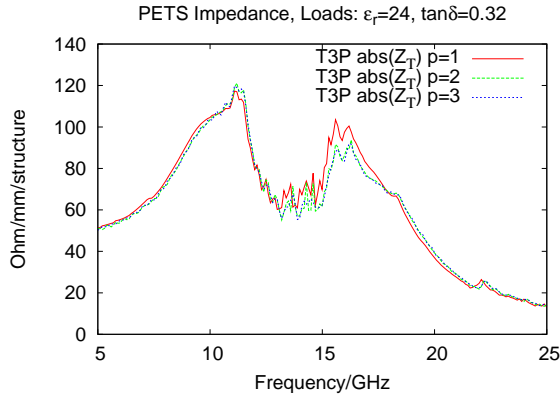


**Figure 6.** Convergence of transverse impedance in the PETs as a function of the order  $p$  of the Finite Element basis functions used in T3P calculations. The impedance is the Fourier transform of the wake potential of a point charge, and is calculated from the transverse wake potential shown in figure 5.

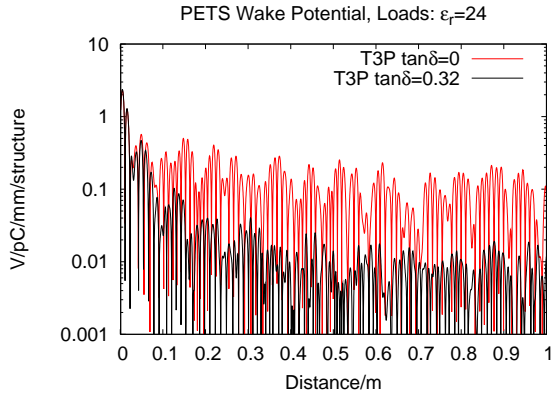


**Figure 7.** Impact of the lossy absorbers on the damping of the transverse wakefields in the PETs. The transverse wake potential for the lossless case ( $\tan\delta=0$ ) is compared to the lossy case ( $\tan\delta=0.32$ ), as calculated with T3P with second-order basis functions ( $p=2$ ).

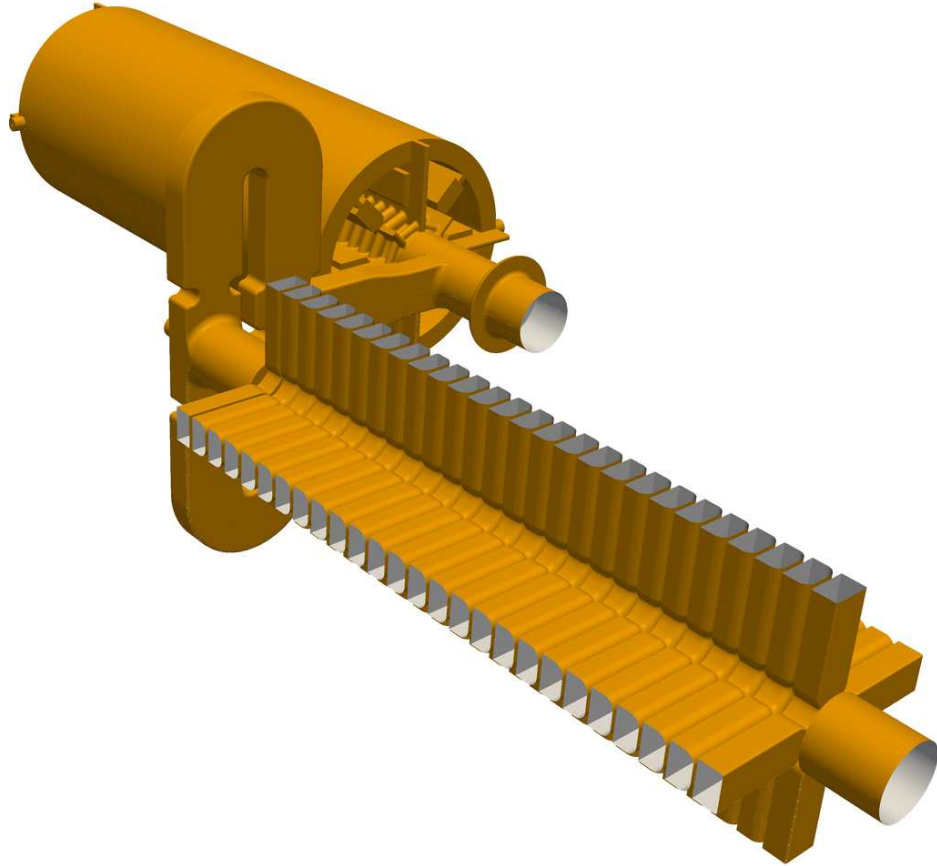
to the accelerating structure is investigated numerically with T3P. The drive beam in the PETs has no transverse offset and excites monopole modes which couple through the output coupler and the connecting waveguides to the accelerating structure. Since the waveguides are specified to have near perfect transmission of the fundamental mode, their detailed layout is not important for the purposes of this study. A quarter model of the PETs is connected to a half model of the accelerating structure, and the use of symmetric (magnetic) boundary conditions leads to one PETs being connected to two accelerating structures – in accordance with the CLIC design.

Figure 9 shows a time sequence of the power flow from the PETs to the accelerating structure. The low group velocity ( $\approx 0.02c$ ) of the accelerating structure leads to an effective pulse compression which produces high gradients. Dispersion effects in the accelerating structure might have led to a broadening of the RF pulse due to the high-frequency content of the single bunch profile, while the current CLIC design uses multiple bunches for the PETs drive beam. Multi-bunch simulations will be performed to verify the two-beam accelerator power transfer scheme.

## 5. Summary

SLAC's parallel 3D electromagnetic time-domain code T3P employs state-of-the-art parallel Finite Element methods on curved conformal unstructured meshes with higher-order field representation. T3P allows large-scale time-domain simulations of complex, realistic 3D structures with unprecedented accuracy, aiding the design and operation of the next generation of accelerator facilities.

T3P was applied to calculate transverse wakefield damping effects in the CLIC power and extraction structure (PETs), and convergence in the results was found. Furthermore, a two-structure time-domain simulation of the power transfer from the PETs to the main CLIC accelerating structures was performed. Future applications will include transverse wakefield coupling effects from the PETs to the accelerating structures. Further code development is necessary to accommodate accurate numerical termination of the waveguides that are essential for wakefield damping.



**Figure 8.** Overview of the coupled model of the PETs (left) and the accelerating structure (right), used for T3P calculations of RF power transfer. An on-axis drive beam in the PETs excites monopole modes in the PETs which are transferred through coupling waveguides to the accelerating structure, a low group-velocity design based on four connected waveguides and slightly detuned cells for operating at high gradients. Each PETs is connected to two accelerating structures, but only one accelerating structure is shown here.

### Acknowledgments

This work was supported by the US DOE ASCR, BES, and HEP Divisions under contract No. DE-AC002-76SF00515. This research used resources of the National Energy Research Scientific Computing Center, and of the National Center for Computational Sciences at Oak Ridge National Laboratory, which are supported by the Office of Science of the U. S. Department of Energy under Contract No. DE-AC02-05CH11231 and No. DE-AC05-00OR22725. – We also acknowledge the contributions from our SciDAC collaborators in numerous areas of computational science and A. Grudiev, I. Syratchev and W. Wuensch from the CLIC RF structure development program at CERN.

### References

- [1] Ainsworth M 2004 Dispersive properties of high-order Nedelec/edge element approximation of the time-harmonic Maxwell equations, *Philos. trans.-Royal Soc., Math. phys. eng. sci.*, **362**, no. 1816
- [2] Gedney S, Navsariwala U 1995 An unconditionally stable finite element time-domain solution of the vector wave equation *Microwave and Guided Wave Letters, IEEE*, **5**, no. 10

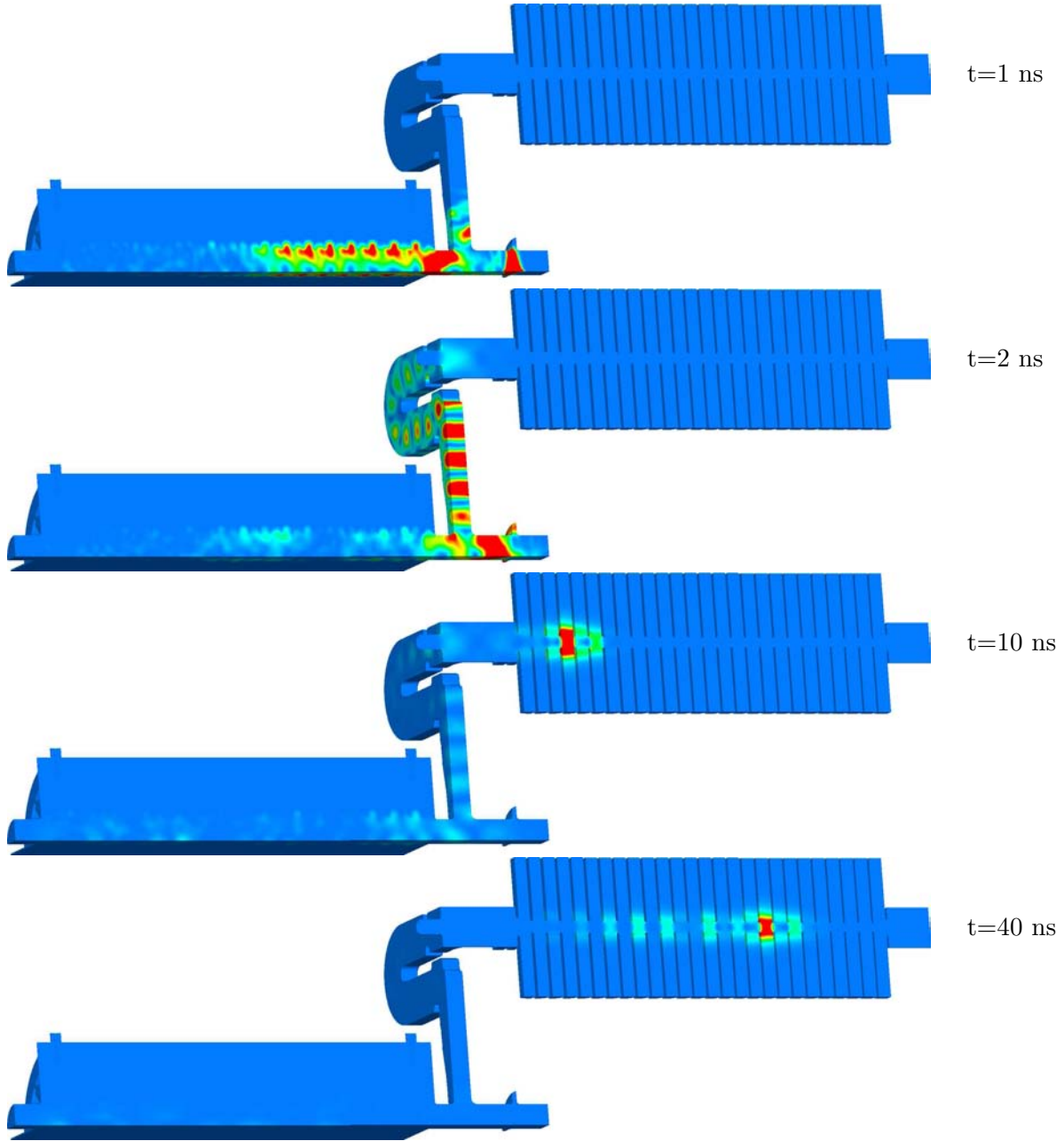


**Figure 9.** Power transfer from the PETs to the main beam accelerating structure, as simulated with T3P ( $p=1$ ) for a single drive bunch. The low group velocity ( $\approx 0.02c$ ) of the accelerating structure leads to an effective pulse compression which produces high gradients.

- [3] Lee L *et al* 2007 Enabling technologies for petascale electromagnetic accelerator simulation *J. Phys.: Conf. Ser.* **78** 012040
- [4] Lee L *et al* 2008 Computational science research in support of petascale electromagnetic modeling *J. Phys.: Conf. Ser.* **125** 012077
- [5] Ng C *et al* 2008 Design and optimization of large accelerator systems through high-fidelity electromagnetic simulations, *J. Phys.: Conf. Ser.* **125** 012003
- [6] Candel A *et al* 2008 Wakefield Computations for the CLIC PETs using the Parallel Finite Element Time-Domain Code T3P, *Proc. X-band RF Structure & Beam Dynamics Workshop*, Cockcroft Institute, UK